Nanoparticle Morphology

International Edition: DOI: 10.1002/anie.201605956
German Edition: DOI: 10.1002/ange.201605956

In Situ Observation of Hydrogen-Induced Surface Faceting for Palladium–Copper Nanocrystals at Atmospheric Pressure

Ying Jiang[+], Hengbo Li[+], Zhemin Wu, Wenying Ye, Hui Zhang, Yong Wang, Chenghua Sun,* and Ze Zhang*

Abstract: *Nanocrystal (NC) morphology, which decides the number of active sites and catalytic efficiency, is strongly determined by the gases involved in synthesis, treatment, and reaction. Myriad investigations have been performed to understand the morphological response to the involved gases. However, most prior work is limited to low pressures, which is far beyond realistic conditions. A dynamic morphological evolution of palladium–copper (PdCu) NC within a nanoreactor is reported, with atmospheric pressure hydrogen at the atomic scale. In situ transmission electron microscopy (TEM) videos reveal that spherical PdCu particles transform into truncated cubes at high hydrogen pressure. First principles calculations demonstrate that the surface energies decline with hydrogen pressure, with a new order of $\gamma_{H\text{-}001} < \gamma_{H\text{-}110} < \gamma_{H\text{-}111}$ at 1 bar. A comprehensive Wulff construction based on the corrected surface energies is perfectly consistent with the experiments. The work provides a microscopic insight into NC behaviors at realistic gas pressure and is promising for the shaping of nanocatalysts by gas-assisted treatments.*

Surface properties of NCs are crucial to catalytic efficiency.[1] In particular, morphology and surface structure are highly dependent on the involved gases. Extensive work has been devoted to studying the influence of gases on NCs during synthesis and usage. For example, researchers utilized gas-assisted methods to facilitate the synthesis of anisotropic and faceted NCs.[2] Furthermore, the as-synthesized structures were found to be largely modified by gases in the post-synthesis treatments and reactive environments.[3] Nolte et al. reported that rhodium NCs underwent an extension of the (001) surface and a reduction of the (111) surface during exposure to 3×10^{-5} mbar oxygen at 600 K.[4] Hansen and co-workers found that the shapes of Cu/ZnO varied with the components of gases during annealing at 220 °C with pressures of several millibars.[5] For bimetallic NCs, Xin et al. showed that in PtCo NCs Co migrated to the surface and finally formed islands in an oxidative environment.[6] Tao et al. demonstrated that stepped platinum surfaces were reconstructed when exposed to CO at pressure above 0.1 torr.[7] The groups of Kooyman and Helveg explored Pt-catalyzed CO oxidation by TEM, and found Pt oscillatory behavior between faceted and spherical terminations.[3d] Nevertheless, because of the tolerance of the equipment to gas pressures, most early studies were performed at ultralow pressures, which cannot truly reflect the real working conditions of NCs. This may become a key issue when a highly reactive gas, such as H_2, is involved. To address this challenge, in situ TEM observations under real reaction conditions are an ideal strategy to establish advanced knowledge regarding the stabilities of NC surfaces.

Our study focuses on PdCu NCs. Palladium is a model catalyst for many reactions, and plays a significant role in almost every aspect of hydrogen-based industries,[8] including hydrogen purification, hydrogenation and dehydrogenation, and methane steam reforming. However, the high cost of Pd hampers large-scale application. Alternatives are desired to reduce costs without a loss of performance; for example, Pd may be alloyed with less expensive transition metals. PdCu has been widely employed as a model Pd-alloy with excellent ligand and ensemble effects, as supported by previous successes.[8e,9] Even so, the response of PdCu NCs to surrounding hydrogen has been poorly investigated, although hydrogen is extensively involved in these reactions, especially at atmospheric pressure.

Herein, we chose to study PdCu NCs during annealing at about 600 K in an atmospheric pressure hydrogen environment. Atom-resolved TEM studies reveal that, although the as-synthesized spherical PdCu NCs are stable when heated at low pressure, they transform into truncated cubes with distinct surface facets at 1 bar hydrogen. First principles calculations clarified that such change is essentially induced by hydrogen; specifically the surface energies of (001), (110), and (111) surfaces vary with hydrogen pressure. With corrected surface energies, a straightforward understanding was provided by Wulff construction for H-terminated PdCu NCs.

The highly monodisperse spherical PdCu NCs were prepared by a modified chemical method reported in a previous work[1a] (see the Supporting Information for details). $Pd(acac)_2$ and $Cu(acac)_2$ precursors were co-reduced in oleylamine, which was mixed with another solution composed of oleylamine and trioctylphosphine oxide (TOPO) and heated at 180 °C for 3 h. The as-synthesized

[*] Y. Jiang,[+] H. Li,[+] Z. Wu, W. Ye, Prof. H. Zhang, Prof. Y. Wang, Prof. Z. Zhang
State Key Laboratory of Silicon Materials and Center of Electron Microscopy, School of Materials Science and Engineering
Zhejiang University
Hangzhou 310027 (China)
E-mail: yongwang@zju.edu.cn
Dr. C. Sun
ARC Centre for Electromaterials Science, School of Chemistry
Monash University
Clayton, Victoria 3800 (Australia)
E-mail: chenghua.sun@monash.edu
[+] These authors contributed equally to this work.

Supporting information for this article can be found under: http://dx.doi.org/10.1002/anie.201605956.

PdCu NCs were dispersed on a SiN film supported across a heating chip. All the heating experiments and in situ observations were carried out by transmission electron microscope (TEM; Tecnai, F20, FEI), with a single-tilt heating gas holder (SGSH30, DENSsolutions) functionalized with electron-transparent windows on the bottom/top chips and heating spiral on the bottom chip.[10] The gas pressures in the reactor were confirmed by both the pressure gauge and monitoring of heating power, as shown in Figure S1 (Supporting Information). High resolution scanning TEM (STEM) analyses, including high-angle annular dark-field (HAADF) images and energy dispersive X-ray spectroscopy (EDX) maps were acquired in vacuum at room temperature, by Cs-corrected TEM (Titan ChemiSTEM, FEI), operating at 200 kV.

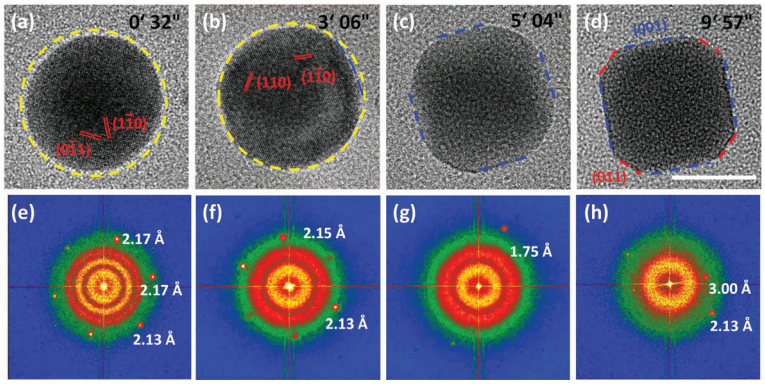

Figure 2. a–d) Lattice-resolved TEM images and the corresponding FFT patterns showing the morphological evolution of the PdCu NC when exposed to H_2 at 1 bar and with heating at 600 K. Scale bar: 10 nm.

The spherical PdCu NCs have an average diameter of 16 nm, as shown in the typical HAADF image in Figure 1 a.

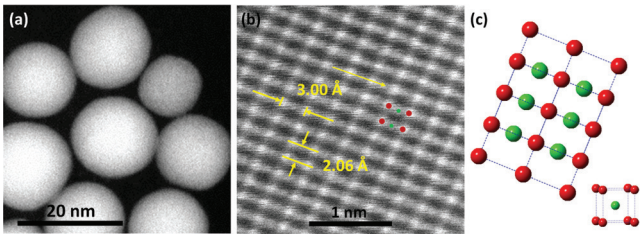

Figure 1. Characterization of PdCu NCs. a) Low magnification and b) high magnification STEM-HAADF images of PdCu NCs. c) Representation of the PdCu crystalline structure, demonstrating that Cu atoms are located at the body center of the primitive Pd matrix. Key: Pd (red), Cu (green).

The ratio between Pd and Cu is 1:1, and Pd/Cu distributes uniformly (Supporting Information, Figure S2). A high resolution HAADF image of a PdCu NC (Figure 1 b) shows a two dimensional atom matrix with d-spacings of approximately 3.00 and 2.06 Å. According to the powder-diffraction file (PDF)-database of the International Centre for Diffraction Data (ICDD), those two facets can be indexed as {100} and {110} of the primitive cubic PdCu NCs. Although Pd and Cu have a face-centered cubic crystalline structure, PdCu is capable of exhibiting a primitive cube (B2) with space group *Pm3m*.[1a,11] Furthermore, the dark and bright contrasts arranged alternately along the yellow arrow indicate a long range chemical ordering, where Cu atoms locate at the body center of the primitive Pd matrix, as shown in the Z (atomic number)-contrast HAADF image of Figure 1 b. The structure schematic projected along [110] is illustrated in Figure 1 c, perfectly consistent with the atomic contrast in Figure 1 b.

The spherical PdCu NCs on a SiN chip were loaded into a sealed gas reactor and exposed to 1 bar H_2. To rule out the effects of NC coalescence or sintering when PdCu NCs were heating at 600 K,[12] the solution was heavily diluted and only one NC appeared in the view during the recording. Figure 2 a displays a TEM image of a single spherical PdCu NC projected along the [111] axis; six {110} diffraction spots can be observed in the corresponding fast Fourier transform (FFT) pattern in Figure 2 e. When annealed at 600 K, the spherical PdCu NC starts to rotate and shows smaller curvature surfaces, as indicated by the blue dashed line in Figure 2 b. Subsequently, accompanied by roll-over and rotation, the NC exhibits four flat surfaces (Figure 2 c) and finally becomes a truncated cube with distinct {001} and {011} facets (Figure 2 d). The FFT patterns of the TEM images are presented in Figures 2 f–h, and the dynamic transformation is recorded in Movie S1 (Supporting Information). Atom distribution of the PdCu cube is still uniform and the volume before and after the transformation fluctuates only by one percent, indicating a main intraparticle mass transport, as shown in Figures S3 and S4 (Supporting Information). Atomically resolved STEM-HAADF images of the PdCu NCs before (sphere) and after (truncated cube) the transformation are shown as insets in Figure 3 (and the Supporting Information, Figure S5), further demonstrating that there is no segregation in the NCs. Another example projected along

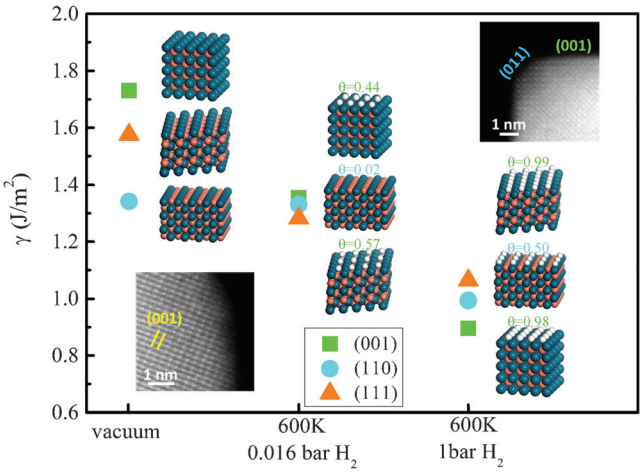

Figure 3. The surface energies and models of (001), (110), and (111) surfaces. Key: Pd (blue), Cu (orange), and H (white). Insets: HAADF images of the surfaces for the spherical and surface-faceted PdCu nanocrystals.

the [111] zone axis is presented in Figure S6 and Movie S2 (Supporting Information). Such surface faceting was not observed at low pressures, such as 0.016 bar H_2, as presented in Figure S7 (Supporting Information).

Consequently, we conclude that the spherical B2 PdCu NCs will transform into truncated cubes when annealed at 600 K in an atmospheric pressure hydrogen environment. To clarify the mechanism of surface faceting, we studied the interaction of PdCu with hydrogen, including absorption into the bulk (solid solution or metal hydride) and adsorption on the surface. We first rule out the possibility of PdCu hydride. It is well-accepted that the critical temperature (T_c) for the co-existence of α solid solution and β hydride is about 570 K (Pd bulk), which is decreased to 430 K for nanocrystals.[13] Above T_c, the α phase becomes dominant at 1 bar H_2. Thus for pure Pd nanocrystals, there is only an α phase at 600 K and 1 bar hydrogen. Furthermore, the α/β-phase transition is accompanied by an increase in H concentration.[13] However, the hydrogen solubility was found to be reduced with Cu concentration by alloying Pd with Cu.[14] Therefore, we can expect that no PdCu hydride will form at 600 K and 1 bar hydrogen. Additionally, we performed test calculations on the possible H_2 absorption or adsorption models, as shown in Figure S8 (Supporting Information). Structure stability and total energies support that H atoms prefer to adsorb on the surface rather than diffuse into the bulk of PdCu.

To further clarify the effect of hydrogen adsorption on the surface faceting, theoretical calculations were performed on the PdCu surface energy with or without hydrogen adsorption. It has been proposed that adsorbate adsorption could largely modify the surface energy in equilibrium by the adsorption energy E_{ads}, and the coverage of atoms (θ), based on pure surface energy (γ_{hkl}), as shown in Equation (1),[15]

$$\gamma_{hkl}^{int} = \gamma_{hkl} + \theta \frac{E_{ads}}{A_{at}} \quad (1)$$

where γ_{hkl} is the (hkl) surface energy of unit area, θ is the surface coverage, E_{ads} is the adsorption energy, and A_{at} is the surface area per surface atom.

γ_{hkl} and θ were acquired by Equations (2) and (3).

$$\gamma = \frac{E_{Pd_NCu_N}^{slab} - N E_{PdCu}^{bulk}}{2A} \quad (2)$$

$$\theta = \frac{pK}{1+pK} \quad (3)$$

Where $E_{Pd_NCu_N}^{slab}$ is the energy for the PdCu slab, E_{PdCu}^{bulk} is the bulk energy of PdCu, A is the (hkl) surface area, T is the temperature, p is gas pressure, and K is the Langmuir isotherm constant, containing the temperature and adsorption energy terms. E_{ads} is acquired by monolayer H adsorption on the Pd-termination model, as discussed in Figure S9 (Supporting Information). Other calculation details are found in the Supporting Information.

Based on Equations (1)–(3), the calculated values (γ_{hkl}, E_{ads}, A_{at}, and θ) of (001), (110), and (111) surfaces are listed in Table S1 (Supporting Information), according to which the surface energies of PdCu NCs under different pressures are extracted, as shown in Table S2 (Supporting Information). The relative stabilities of different surfaces are presented in Figure 3 in terms of specific surface energies, which clearly shows that, the surface will be heavily hydrogenated at the hydrogen pressure of 1 bar, leading to a new order of the surface energies, $\gamma_{H\text{-}001}$ (0.90 J m^{-2}) < $\gamma_{H\text{-}110}$ (0.99 J m^{-2}) < $\gamma_{H\text{-}111}$ (1.06 J m^{-2}). A comprehensive Wulff construction was developed by assuming that only those low-index facets are exposed on the PdCu NCs. Based on the surface energies at 1 bar H_2, a three dimensional configuration of PdCu NC was reconstructed in Figure 4, which shows perfect consistency with our experiments, both from the [100] and [111] zone axes.

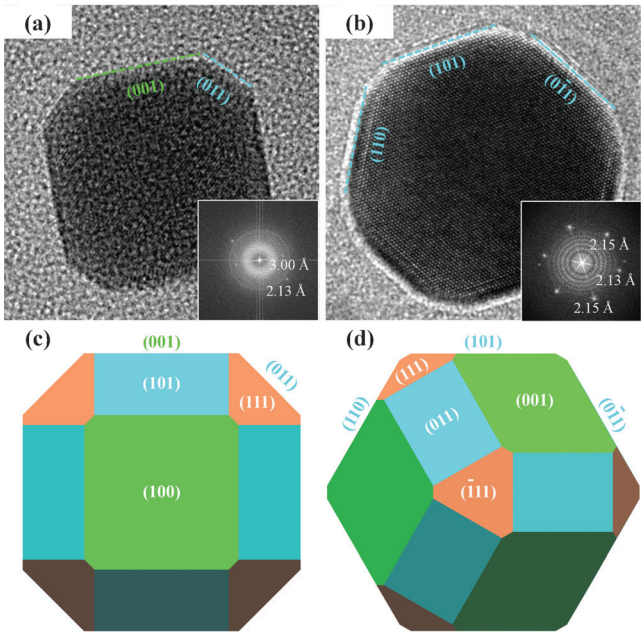

Figure 4. TEM images and Wulff constructions of the PdCu NCs projected from specific directions: a) and c) [100]; b) and d) [111].

Besides such thermodynamic factors, adsorbed hydrogen promoting surface diffusion also plays a significant role in the transformation,[16] which is supported by the fact that the PdCu NCs retain the as-synthesized shape (round) when heating in vacuum (10^{-7} bar) at 600 K. Moreover, when the PdCu NCs were exposed to 0.016 bar at 600 K, the surface energies of (001), (110), and (111) decreased but were quite close, thus the PdCu NCs prefer to retain the as-synthesized spherical morphology.

In conclusion, using a sealed gas reactor we recorded the in situ surface faceting of PdCu NCs under a hydrogen environment at atmospheric pressure. Combined with theoretical calculations, it is clarified that the surface faceting essentially results from hydrogen termination, which can remarkably improve the stability of (001). Traditionally, the characterization of nanocatalysts is performed under vacuum or ultralow pressures, resulting in a knowledge gap with real applications at atmospheric pressure. Our work demonstrates that gas nanoreactors can effectively fill this gap. This study conceptualizes the use of simple post-synthesis treatments to achieve the surface faceting of alloyed NPs, thereby

facilitating the tailoring of their physical and chemical properties for catalytic applications.

Acknowledgements

We acknowledge the support of the National Natural Science Foundation of China (51390474, 11234011, 11327901), the Ministry of Education of China (IRT13037) and National Young 1000 Talents Program of China. C.S. acknowledges financial support from ARC Discover Project (DP130100268) and Future Fellowship (FT130100076). C.S. appreciates the generous grants of CPU time from Australian National Computational Infrastructure and MASSIVE HPC. We thank Prof. Y. Gao at Shanghai Institute of Applied Physics, Chinese Academy of Sciences, for the helpful discussions regarding the calculations.

Keywords: metal–hydrogen interactions · palladium–copper nanoparticles · surface faceting · Wulff construction

How to cite: *Angew. Chem. Int. Ed.* **2016**, *55*, 12427–12430
Angew. Chem. **2016**, *128*, 12615–12618

[1] a) Q. Gao, Y.-M. Ju, D. An, M.-R. Gao, C.-H. Cui, J.-W. Liu, H.-P. Cong, S.-H. Yu, *ChemSusChem* **2013**, *6*, 1878; b) H. Lee, S. E. Habas, S. Kweskin, D. Butcher, G. A. Somorjai, P. Yang, *Angew. Chem. Int. Ed.* **2006**, *45*, 7824; *Angew. Chem.* **2006**, *118*, 7988; c) L. Wang, S. Zhao, C. Liu, C. Li, X. Li, H. Li, Y. Wang, C. Ma, Z. Li, J. Zeng, *Nano Lett.* **2015**, *15*, 2875.

[2] a) Y. Dai, X. Mu, Y. Tan, K. Lin, Z. Yang, N. Zheng, G. Fu, *J. Am. Chem. Soc.* **2012**, *134*, 7073; b) T. S. Ahmadi, Z. L. Wang, T. C. Green, A. Henglein, M. A. El-Sayed, *Science* **1996**, *272*, 1924; c) J. Ren, R. D. Tilley, *Small* **2007**, *3*, 1508.

[3] a) F. Gao, Y. Wang, D. W. Goodman, *J. Phys. Chem. C* **2009**, *113*, 14993; b) L.-L. Wang, T. L. Tan, D. D. Johnson, *Nano Lett.* **2014**, *14*, 7077; c) M. Chi, C. Wang, Y. Lei, G. Wang, D. Li, K. L. More, A. Lupini, L. F. Allard, N. M. Markovic, V. R. Stamenkovic, *Nat. Commun.* **2015**, *6*, 8925; d) S. B. Vendelbo, C. F. Elkjær, H. Falsig, I. Puspitasari, P. Dona, L. Mele, B. Morana, B. J. Nelissen, R. van Rijn, J. F. Creemer, P. J. Kooyman, S. Helveg, *Nat. Mater.* **2014**, *13*, 884; e) W. Yuan, Y. Wang, H. Li, H. Wu, Z. Zhang, A. Selloni, C. Sun, *Nano Lett.* **2016**, *16*, 132; f) Y. A. Wu, L. Li, Z. Li, A. Kinaci, M. K. Y. Chan, Y. Sun, J. R. Guest, I. McNulty, T. Rajh, Y. Liu, *ACS Nano* **2016**, *10*, 3738; g) H. Li, W. Yuan, Y. Jiang, Z. Zhang, Z. Zhang, Y. Wang, *Prog. Nat. Sci.: Mater. Int.* **2016**, *26*, 308; h) E. de Smit, I. Swart, J. F. Creemer, C. Karunakaran, D. Bertwistle, H. W. Zandbergen, F. M. F. de Groot, B. M. Weckhuysen, *Angew. Chem. Int. Ed.* **2009**, *48*, 3632; *Angew. Chem.* **2009**, *121*, 3686; i) H. Yoshida, Y. Kuwauchi, J. R. Jinschek, K. J. Sun, S. Tanaka, M. Kohyama, S. Shimada, M. Haruta, S. Takeda, *Science* **2012**, *335*, 317; j) S. Y. Zhang, P. N. Plessow, J. J. Willis, S. Dai, M. J. Xu, G. W. Graham, M. Cargnello, F. Abild-Pedersen, X. Q. Pan, *Nano Lett.* **2016**, *16*, 4528; k) A. Baldi, T. C. Narayan, A. L. Koh, J. A. Dionne, *Nat. Mater.* **2014**, *13*, 1143.

[4] P. Nolte, A. Stierle, N. Y. Jin-Phillipp, N. Kasper, T. U. Schulli, H. Dosch, *Science* **2008**, *321*, 1654.

[5] P. L. Hansen, J. B. Wagner, S. Helveg, J. R. Rostrup-Nielsen, B. S. Clausen, H. Topsøe, *Science* **2002**, *295*, 2053.

[6] H. L. Xin, S. Alayoglu, R. Tao, A. Genc, C.-M. Wang, L. Kovarik, E. A. Stach, L.-W. Wang, M. Salmeron, G. A. Somorjai, H. Zheng, *Nano Lett.* **2014**, *14*, 3203.

[7] F. Tao, S. Dag, L.-W. Wang, Z. Liu, D. R. Butcher, H. Bluhm, M. Salmeron, G. A. Somorjai, *Science* **2010**, *327*, 850.

[8] a) B. D. Adams, A. Chen, *Mater. Today* **2011**, *14*, 282; b) R. Dittmeyer, V. Hollein, K. Daub, *J. Mol. Catal. A* **2001**, *173*, 135; c) Y. Bi, H. Xu, W. Li, A. Goldbach, *Int. J. Hydrogen Energy* **2009**, *34*, 2965; d) J. Shu, B. P. A. Grandjean, S. Kaliaguine, *Appl. Catal. A* **1994**, *119*, 305; e) X. Jiang, N. Koizumi, X. Guo, C. Song, *Appl. Catal. B* **2015**, *170*, 173.

[9] a) J. Mao, Y. Liu, Z. Chen, D. Wang, Y. Li, *Chem. Commun.* **2014**, *50*, 4588; b) K.-H. Park, Y. W. Lee, S. W. Kang, S. W. Han, *Chem. Asian J.* **2011**, *6*, 1515; c) E. B. Fox, S. Velu, M. H. Engelhard, Y.-H. Chin, J. T. Miller, J. Kropf, C. Song, *J. Catal.* **2008**, *260*, 358; d) B. Jiang, C. Li, V. Malgras, Y. Bando, Y. Yamauchi, *Chem. Commun.* **2016**, *52*, 1186; e) M.-W. Hsieh, T.-J. Whang, *Appl. Surf. Sci.* **2013**, *270*, 252.

[10] J. F. Creemer, S. Helveg, G. H. Hoveling, S. Ullmann, A. M. Molenbroek, P. M. Sarro, H. W. Zandbergen, *Ultramicroscopy* **2008**, *108*, 993.

[11] a) M. Yamauchi, T. Tsukuda, *Dalton Trans.* **2011**, *40*, 4842; b) C. Wang, D. P. Chen, X. Sang, R. R. Unocic, S. E. Skrabalak, *ACS Nano* **2016**, *10*, 6345.

[12] Y. Jiang, Y. Wang, Y. Zhang, Z. Zhang, W. Yuan, C. Sun, X. Wei, C. Brodsky, C.-K. Tsung, J. Li, X. Zhang, S. Mao, S. Zhang, Z. Zhang, *Nano Res.* **2014**, *7*, 308.

[13] D. G. Narehood, S. Kishore, H. Goto, J. H. Adair, *Int. J. Hydrogen Energy* **2009**, *34*, 952.

[14] S. M. Opalka, W. Huang, D. Wang, T. B. Flanagan, O. M. Lovvik, S. C. Emerson, Y. She, T. H. Vanderspurt, *J. Alloys Compd.* **2007**, *446*, 583.

[15] B. Zhu, Z. Xu, C. Wang, Y. Gao, *Nano Lett.* **2016**, *16*, 2628.

[16] a) G. L. Kellogg, *Phys. Rev. B* **1997**, *55*, 7206; b) S. Horch, H. T. Lorensen, S. Helveg, E. Laegsgaard, I. Stensgaard, K. W. Jacobsen, J. K. Norskov, F. Besenbacher, *Nature* **1999**, *398*, 134.

Received: June 20, 2016
Revised: July 25, 2016
Published online: September 4, 2016

